DOI: 10.1002/chem.200501041

A Family of Ferro- and Antiferromagnetically Coupled Decametallic Chromium(III) Wheels

David M. Low,[a] Gopalan Rajaraman,[a] Madeleine Helliwell,[a] Grigore Timco,[a] Joris van Slageren,[b] Roberta Sessoli,[c] Stefan T. Ochsenbein,[d] Roland Bircher,[d] Christopher Dobe,[d] Oliver Waldmann,[d] Hans-Ulrich Güdel,[d] Mark A. Adams,[e] Eliseo Ruiz,[f] Santiago Alvarez,[f] and Eric J. L. McInnes*[a]

Abstract: The synthesis and crystal structures of a family of decametallic Cr^{III} "molecular wheels" are reported, namely $[Cr_{10}(OR)_{20}(O_2CR')_{10}]$ [R′ = Me, R = Me (**1**), Et (**2**); R′ = Et, R = Me (**3**), Et (**4**); R′ = CMe_3, R = Me (**5**), Et (**6**)]. Magnetic studies on **1**–**6** reveal a remarkable dependence of the magnetic behaviour on the nature of R. In each pair of complexes with a common carboxylate (R′) the nearest neighbour Cr···Cr magnetic exchange coupling is more antiferromagnetic for the ethoxide-bridged (R = Et) cluster than for the methoxide analogue. In complexes **2**, **4** and **6** the overall coupling is weakly antiferromagnetic resulting in diamagnetic ($S = 0$) ground states for the cluster, whilst in **1** and **5** it is weakly ferromagnetic thus resulting in very high-spin ground states. This ground state has been probed directly in the perdeuterated version of **1** ([D]**1**) by inelastic neutron scattering experiments, and these support the $S = 15$ ground state expected for ferromagnetic coupling of ten Cr^{III} ions, and they also indicate that a single *J*-value model is inadequate. The ground state of **5** is large but not well defined. The trends in *J* on changing R are further supported by density functional calculations on **1**–**6**, which are in excellent agreement with experiment. The very large changes in the nature of the ground state between **1** and **2**, and **5** and **6** are the result of relatively small changes in *J* that happen to cross $J = 0$, hence changing the sign of *J*.

Keywords: chromium · cluster compounds · magnetic properties · metal–metal interactions · solvothermal synthesis

Introduction

The magnetic properties of cyclic, polymetallic complexes of paramagnetic transition-metal ions have attracted great interest. Antiferromagnetically coupled examples are relatively common,[1] and examples are known with nuclearities up to 24.[2] Such molecules are finite models for 1D antiferromagnetic materials,[3] and heterometallic examples[4] have been proposed as good candidates for observing quantum coherence phenomena,[5a] and even as qubits in quantum computing.[5b] However, ferromagnetically coupled cyclic clusters are much rarer. To the best of our knowledge only four have been reported to date, the Cu^{II}_6 and Mn^{III}_6 wheels of Gatteschi and co-workers,[6] and Winpenny's isostructural

[a] Dr. D. M. Low, Dr. G. Rajaraman, Dr. M. Helliwell, Dr. G. Timco, Dr. E. J. L. McInnes
School of Chemistry, The University of Manchester
Manchester M13 9PL (UK)
Fax: (+44) 161-275-4469
E-mail: eric.mcinnes@manchester.ac.uk

[b] Dr. J. van Slageren
1. Physikalisches Institut, Universität Stuttgart
Pfaffenwaldring 57, 70550 Stuttgart (Germany)

[c] Prof. R. Sessoli
Dipartimento di Chimica, Università di Firenze, and UdR INSTM, Via della Lastruccia 3
Sesto Fiorentino (Italy)

[d] S. T. Ochsenbein, R. Bircher, C. Dobe, Dr. O. Waldmann, Prof. H.-U. Güdel
Department of Chemistry and Biochemistry
University of Bern, Freiestrasse 3
3000 Bern 9 (Switzerland)

[e] Dr. M. A. Adams
CCLRC, Rutherford Appleton Laboratory
Chilton, OX11 0QX (UK)

[f] Prof. E. Ruiz, Prof. S. Alvarez
Departament de Química Inorgànica and Centre de Recerca en Química Teòrica (CeRQT)
Universitat de Barcelona, Diagonal 647
08028, Barcelona (Spain)

Ni^{II}_{12} and Co^{II}_{12} pair.[7] Such ferromagnetic coupling leads to a high-spin ground state and the possibility of being a "single molecule magnet" (SMM), in which individual molecules display a memory effect.[8] Indeed the $S=12$ ground state Ni_{12} wheel has been shown to be a SMM.[9]

We recently reported the synthesis (by a solvothermal route) of two decametallic Cr^{III} wheels $[Cr_{10}(OR)_{20}(O_2CMe)_{10}]$, in which R = Me (**1**) or Et (**2**) (with structures analogous to that in Figure 1).[10] These are the highest nuclearity cyclic Cr^{III} clusters reported to date (the highest nuclearity Cr^{III} cluster reported of any structural type is 12),[11] and are analogues of the famous "ferric wheel" $[Fe_{10}(OMe)_{20}(O_2CCH_2Cl)_{10}]$ first prepared by Lippard and co-workers.[12] (The direct analogue of **1**, $[Fe_{10}(OMe)_{20}(O_2CMe)_{10}]$, was reported later by Winpenny and co-workers.[13]) More recently we have also prepared the vanadium(III) analogues.[14] Preliminary magnetic susceptibility studies on **1** and **2** indicated that the magnetic coupling between neighbouring Cr^{III} ions in **2** was antiferromagnetic, as is the case for all other cyclic Cr^{III} complexes reported to date (Cr_{3-8}),[15] albeit the exchange $H=\Sigma -J_{ij}\hat{S}_i\hat{S}_j$, $J=-0.9\ cm^{-1}$ assuming a single unique J value; throughout this paper a negative J value implies an antiferromagnetic interaction) is much weaker in comparison. This of course leads to an $S=0$ ground state, since there is an even number of paramagnetic ions in the ring. Remarkably, χT (χ = molar magnetic susceptibility, T = temperature) increased with decreasing temperature for the methoxide analogue **1** showing that it is ferromagnetically coupled (see data in Figure 3, later). Unfortunately, analysis of the magnetic data was hampered by the presence of a significant antiferromagnetic intermolecular exchange that caused χT to collapse at low temperatures. Modelling of the χT versus T data of **2** gave an intramolecular exchange $J=+4.5\ cm^{-1}$, with $J_{inter}=-0.26\ cm^{-1}$.[10] If this model is correct then the ground-state spin of **1** must be $S=15$, which would be among the highest known for any molecule.[16] Hence, it appears that a trivial change in the chemistry (ethoxide vs methoxide bridge) leads to a small change in the magnitude of J (J changes by $5.4\ cm^{-1}$); however, because the sign of J changes there is a monumental change in the nature of the ground state: $S=0$ to $S=15$.

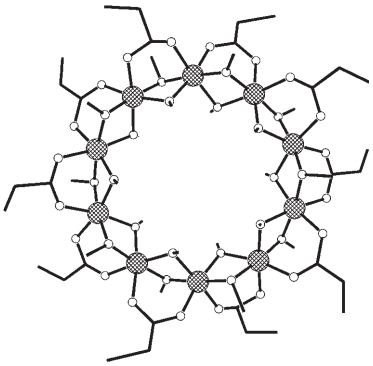

Figure 1. Molecular structure of $[Cr_{10}(OMe)_{20}(O_2CEt)_{10}]$ (**3**), viewed perpendicular to the best plane of the Cr_{10} ring. Scheme: Cr (cross hatched), O (open circles), C (skeleton only), H omitted for clarity.

To probe this further we set out to prepare further examples of this family of complexes in the hope of developing a magnetostructural correlation. As a further goal we wished to prepare analogues of **1** and **2** in which the molecules could be magnetically isolated to a greater extent to reduce any possible intermolecular exchange or dipolar interactions. This entails incorporating bulkier carboxylate and/or alkoxide groups into the molecules with the aim of spacing them further apart in the crystal lattice. We now report the synthesis of bulkier analogues of **1** and **2**, namely $[Cr_{10}(OR)_{20}(O_2CEt)_{10}]$ [R = Me (**3**), Et (**4**)] and $[Cr_{10}(OR)_{20}(O_2CCMe_3)_{10}]$ [R = Me (**5**), Et (**6**)], and their structural and magnetic characterisation, including the second example of a ferromagnetically coupled Cr_{10} wheel (compound **5**). The experimental observation of ferromagnetic coupling in rings **1** and **5**, is supported by density functional theory (DFT) calculations on **1**–**6**, and confirmed by the direct measurement of J in the fully deuterated analogue of compound **1** ([D]**1**) by inelastic neutron scattering (INS).

Results and Discussion

Synthesis: As part of a programme investigating the use of solvothermal synthetic techniques towards large paramagnetic clusters,[17] we previously described the synthesis of the decametallic Cr^{III} complexes $[Cr_{10}(OR)_{20}(O_2CMe)_{10}]$ by superheating alcohol [ROH; R = Me (**1**), Et (**2**)] solutions of the trinuclear basic chromium acetate $[Cr_3O(O_2CMe)_6(H_2O)_3]Cl$ at 200 °C.[10] Analogous reactions with $[Cr_3O(O_2CEt)_6(H_2O)_3]NO_3$ give the propionate analogues $[Cr_{10}(OR)_{20}(O_2CEt)_{10}]$ [R = Me (**3**), Et (**4**)] in excellent yields with the products crystallising directly from the reaction mixtures. However, similar treatments of the pivalate complex $[Cr_3O(O_2CCMe_3)_6(H_2O)_3]NO_3$ fail to crystallise any products on cooling the reaction mixtures, possibly because the reaction intermediates and products are too soluble in ROH. However, in a (failed) attempt to synthesise an alkoxide-bridged octametallic wheel by reaction of $[Cr_8F_8(O_2CCMe_3)_{16}]$[18] in superheated MeOH, the decametallic pivalate wheel $[Cr_{10}(OMe)_{20}(O_2CCMe_3)_{10}]$ (**5**) crystallised in good yield. We originally used a solution of $[Cr_8F_8(O_2CCMe_3)_{16}]$ in a toluene/MeOH mixture, as the starting material is not soluble in MeOH but it is in toluene. However, we then discovered that simply heating a mixture of the starting material and MeOH at 200 °C also gave pure crystalline product **5** in improved yield. This highlights one of the advantages of solvothermal techniques in the synthesis of clusters—the changed solubilising properties of the solvent under superheated conditions allows this reaction to take place. A similar reaction of a mixture of $[Cr_8F_8(O_2CCMe_3)_{16}]$ and EtOH gives $[Cr_{10}(OEt)_{20}(O_2CCMe_3)_{10}]$ (**6**).

In contrast to the insoluble complexes **1** and **2**,[10] complexes **3**–**6** are very soluble in a variety of organic solvents,

and their integrity in solution is confirmed by the presence of the molecular ion in electrospray mass spectrometry.

Compound [D]**1** was prepared by reaction of $[Cr_3O(O_2CD_3)_6(H_2O)_3](O_2CCD_3)$ in CD_3OD at 200 °C. We found that this route gave higher yields than using a directly analogous reaction to that reported previously for **1**. Note that we only had to use two deuterated reagents in the preparation of [D]**1** (CD_3CO_2D and CD_3OD)—the excess of both of which can be recovered and recycled in order to make the approximate 4 g quantity necessary for INS studies at reasonable cost.

X-ray crystal structures: Unit-cell details for **3–6** are in Table 1. The molecular structures of **3–6** are closely related to the reported structures of **1** and **2**,[10] all consisting of a cyclic, decametallic array of Cr^{III} ions, in which each pair of Cr^{III} ions is bridged by a μ_2-carboxylate and two μ_2-alkoxides (Figure 1). In each case the Cr_{10} ring is near planar (mean square deviations from best planes in Table 3, below). The carboxylate groups alternate between lying above the Cr_{10} plane and below it, but are all oriented away from the centre of the ring. The two alkoxides between each neighbouring pair of Cr^{III} ions point towards and away from the ring, respectively, with one lying above and the other lying below the Cr_{10} plane; this pattern alternates around the ring. Although, the diameter of the Cr_{10} ring is about 9.7 Å in each case, the alkoxide bridges leave little room for any "guest" and the cavities are empty. There is no solvent incorporated in any of the structures.

Compounds **3** and **5** crystallise in $P\bar{1}$ and the molecules lie on an inversion centre, hence there are only five independent Cr^{III} ions in each structure. Compound **4** crystallises in $P2_1/n$ and the molecules lie on a twofold axis: again there are only five independent Cr^{III} ions per molecule. Compound **6** crystallises in $C2/m$ and the molecules lie on a $2m$ site with C_{2h} point symmetry; there are only three independent Cr^{III} ions per molecule. Values for the Cr-O(R)-Cr angles and Cr–Cr separations for **1–6** are in Table 2; the ranges and averages of the important structural parameters for each of **1** to **6** are in Table 3. The Cr···O bond lengths are unremarkable. The Cr-O(R)-Cr interbond angles in **1** to **6** lie between 98 and 100°, with the exception of **3**, which has a range of 95–102°, although the ranges for each individual compound are 1.3–2.5° (7.2° for **3**). There is no significant difference between the average angles for the OR groups that point towards and away from the centre of the rings. The smallest average Cr-O(R)-Cr angle is found for cluster **5** at 98.6 ± 0.6°, while the largest is found for **4** at 99.6 ± 1.3°. The spread of these values makes meaningful comparison of the average structural parameters difficult. There is a significant variation in the Cr···Cr distances in compounds **1** to **6**; the largest average separation is found for **4** (3.028 ± 0.008 Å), while the shortest is found for **6** (2.956 ± 0.006 Å). The spread of the Cr···Cr distances within a given complex is 0.005–0.016 Å.

The molecules pack in a columnar fashion. For complexes **1**, **4**, **5**, and **6** the Cr_{10} rings are significantly tilted with respect to the stacking direction, whilst in complexes **2** and **3** they are nearer perpendicular (e.g., Figure 2); the stacking directions are parallel to the shortest unit-cell axis (*a* in **1–5**, *c* in **6**). The shortest intermolecular distances (measured from the centroids of the Cr_{10} rings) are along these colum-

Table 1. X-ray data for **3–6**.

	3	**4**	**5**	**6**
chemical formula	$Cr_{10}C_{50}H_{110}O_{40}$	$Cr_{10}C_{70}H_{150}O_{40}$	$Cr_{10}C_{70}H_{150}O_{40}$	$Cr_{10}C_{90}H_{190}O_{40}$
M_r	1871.38	2151.90	2151.90	2432.42
crystal dimensions [mm^{-1}]	0.45 × 0.08 × 0.05	0.3 × 0.25 × 0.08	0.30 × 0.30 × 0.20	0.60 × 0.60 × 0.40
crystal system	triclinic	monoclinic	triclinic	monoclinic
space group	$\bar{P}1$ (no. 2)	$P2_1/n$ (no. 14)	$\bar{P}1$ (no. 2)	$C2m$
a [Å]	7.739(10)	9.46(2)	9.867(2)	19.247(14)
b [Å]	17.75(3)	16.87(1)	16.990(2)	32.51(2)
c [Å]	17.71(3)	30.88(5)	17.898(2)	9.347(7)
α [°]	110.22(7)	90	115.098(2)	90
β[°]	102.39(7)	93.07(9)	99.908(2)	103.438(13)
γ[°]	102.48(8)	90	97.185(2)	90
V [Å]	2115(6)	4920(11)	2609.8(7)	5704(7)
Z	1	2	1	2
ρ_{calcd} [$Mg\,m^{-3}$]	1.469	1.453	1.367	1.416
T [K]	293	293	100	100
$2\theta_{max}$ [°]	50.04	50.08	52.84	52.56
data collected	33777	76138	14993	12879
(unique)	(6526)	(7749)	(10396)	(5134)
data used [$I > 2\sigma(I)$]	4989	4959	7679	3520
parameters	451	384	646	315
R (F)	0.1329	0.0878	0.0642	0.0772
wR_2	0.3846	0.2897	0.1725	0.2038
$\Delta\rho_{min}$ [$e\,Å^{-3}$]			−0.641	−0.642
$\Delta\rho_{max}$ [$e\,Å^{-3}$]			0.815	0.841

Table 2. Cr-O(R)-Cr angles [°] and Cr···Cr distances [Å] for **1**–**6**.

	1[a]	**2**[a]	**3**	**4**	**5**	**6**[c]
Cr1-O-Cr2	99.4(3), 99.9(3)	99.2(3), 99.6(3)	100.9(6), 101.9(6)	99.9(2), 100.2(2)	98.3(1), 98.9(2)	99.3(2), 98.6(2)
Cr6-O-Cr7[b]	99.1(3), 98.8(3)					
Cr2-O-Cr3	98.5(3), 98.8(3)	99.1(3), 98.5(3)	97.4(6), 95.2(5)	100.3(2), 99.9(2)	98.0(2), 99.3(2)	99.9(2), 98.3(2)
Cr7-O-Cr8[b]	99.5(3), 99.4(3)					
Cr3-O-Cr4	99.4(3), 98.0(3)	99.3(3), 100.1(3)	98.3(4), 98.7(4)	99.2(2), 99.5(2)	98.3(2), 99.1(2)	
Cr8-O-Cr9[b]	99.9(3), 99.3(4)					
Cr4-O-Cr5	99.3(3), 100.3(4)	99.5(3), 99.4(3)	99.8(5), 102.4(6)	99.2(2), 97.7(2)	98.7(2), 98.5(1)	
Cr9-O-Cr10[b]	99.3(3), 100.1(4)					
Cr5-O-Cr1b	98.9(3), 98.8(3)	98.9(3), 98.8(3)	95.9(5), 98.0(6)	99.1(2), 100.2(2)	98.1(2), 99.0(2)	
Cr10-O-Cr6b[b]	98.9(3), 98.4(3)					
Cr1···Cr2	2.989(3)	2.997(2)	3.009(5)	3.027(2)	2.967(1)	2.950(2)
Cr6···Cr7[b]	2.994(3)					
Cr2···Cr3	2.991(3)	2.992(2)	3.008(5)	3.031(1)	2.966(1)	2.962(2)
Cr7···Cr8[b]	2.989(3)					
Cr3···Cr4	2.984(3)	2.996(2)	2.993(4)	3.034(1)	2.966(1)	
Cr8···Cr9[b]	2.989(3)					
Cr4···Cr5	2.989(3)	2.994(2)	2.996(5)	3.028(1)	2.969(1)	
Cr9···Cr10[b]	2.990(3)					
Cr5···Cr1b	2.988(3)	2.997(2)	3.000(5)	3.018(2)	2.961(1)	
Cr10···Cr6b[b]	2.989(3)					

[a] Reference [10]. [b] Compound **1** has two half molecules per asymmetric unit, Cr1–5 and Cr6–7, respectively. Compounds **2**–**5** have one half molecule per asymmetric unit (Cr1–Cr5); [c] Compound **6** has only three unique Cr^{III} ions (Cr1–Cr3).

Table 3. Structural parameter ranges and averages for **1**–**6**.

	1	**2**	**3**	**4**	**5**	**6**
Cr···Cr [Å]	2.985(3)–2.994(3)	2.992(2)–2.997(2)	2.993(4)–3.009(5)	3.018(2)–3.034(1)	2.961(1)–2.967(1)	2.950(2)–2.962(2)
average [Å]	2.989 ± 0.005	2.995 ± 0.003	3.001 ± 0.008	3.028 ± 0.008	2.966 ± 0.003	2.956 ± 0.006
Cr-O(R)-Cr [°]	98.0(3)-100.3(4)	98.5(3)-100.1(3)	95.2(5)-102.4(6)	97.7(2)-100.3(2)	98.02(15)-99.28(15)	98.3(2)-99.9(2)
average [°]	99.2 ± 0.1	99.2 ± 0.8	98.9 ± 3.6	99.6 ± 1.3	98.6 ± 0.6	99.0 ± 0.9
Cr−O(R) [Å]	1.935(7)–1.985(8)	1.951(6)–1.980(6)	1.893(13)–2.059(11)	1.956(5)–2.024(5)	1.945(3)–1.967(3)	1.927(4)–1.963(5)
Cr−O(carboxylate) [Å]	1.969(8)–2.005(7)	1.981(7)–1.998(7)	1.949(16)–2.055(13)	1.987(5)–2.025(5)	1.973(4)–1.987(3)	1.962(5)–1.982(4)
Cr_{10}···Cr_{10} [Å]	8.83	9.45	7.74	9.46	9.87	9.37
mean deviation from best Cr_{10} plane [Å]	0.0151, 0.0194	0.0116	0.0102	0.0078	0.0078	0.0203

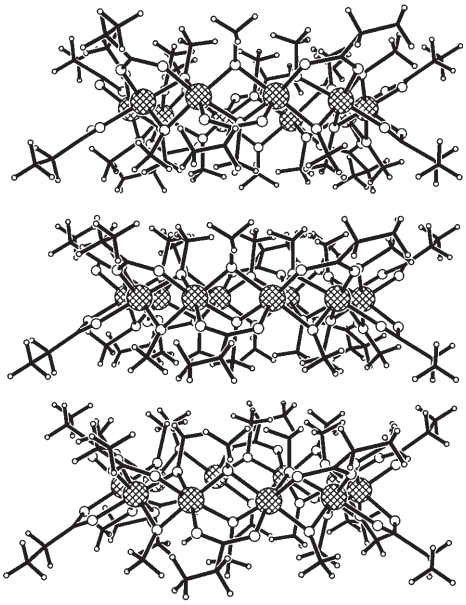

Figure 2. Packing of the molecules in $[Cr_{10}(OMe)_{20}(O_2CEt)_{10}]$ (**3**) viewed perpendicular to the crystallographic *a* axis. Scheme as in Figure 1, but with H atoms shown as small white spheres.

nar directions. The change between acetate (complexes **1** and **2**) and propionate (complexes **3** and **4**) does not significantly alter this separation; the two ethoxide complexes **2** and **4** both stack approximately 9.45 Å apart, whilst the methoxide complexes **1** and **3** pack closer at 8.83 and 7.74 Å, respectively. In these four complexes the nature of the alkoxide seems more important in determining this distance than the carboxylates; the steric bulk above and below the plane of the molecules, which determines the closest intermolecular separations, is due primarily to the alkoxides (e.g., see Figure 2). Although the intermolecular separation in the much bulkier pivalate methoxide complex **5** (9.87 Å) is significantly greater than for the other methoxide complexes **1** and **3** that in the pivalate ethoxide **6** (9.37 Å) is counter-intuitively smaller than that in the other ethoxide complexes **2** and **4**.

Magnetic studies: The magnetic susceptibility as a function of temperature was measured for complexes **3**–**6**; the data are shown as a χT versus T plot in Figure 3, together with the data of **1** for comparison.

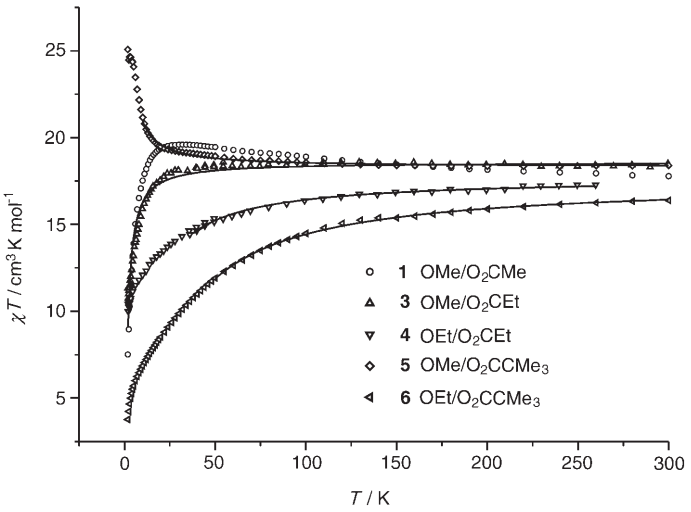

Figure 3. Plots of χT versus T for $[Cr_{10}(OR)_{20}(O_2CR')_{10}]$ [R′=Me, R=Me (**1**); R′=Et, R=Me (**3**), Et (**4**); R′=CMe, R=Me (**5**), Et (**6**)]. Solid lines are best fits as described in the text and using parameters in Table 4.

reason, the fits were not performed down to the lowest temperatures in all cases.

Although, the twofold symmetry of **1**–**5** implies that there are strictly five unique nearest neighbour J values (two unique values in the higher symmetry complex **6**), we have restricted ourselves to a single J model to avoid over-parameterisation. Furthermore, in some cases we have tested the effect of the inclusion of more than one unique J value and there is no significant improvement in the quality of the fits to the experimental χT versus T data (see below); therefore, there is no justification for the use of these more complicated models when fitting χT.

The sign and magnitude of J can also be estimated from Weiss constants (Θ) extracted from Curie–Weiss plots (χ^{-1} vs T). The Weiss constants for **1** and **5** are positive (consistent with ferromagnetic coupling), while those for **2**, **4** and **6** are negative (consistent with antiferromagnetic coupling) and that for **3** is very close to zero (Table 4). The Weiss constants can be related to the nearest neighbour exchange interaction[15c] by Equation (1), in which S_{Cr} is the spin of the Cr^{III} ions (=3/2), k is the Boltzmann constant, and the summation is over nearest neighbours (i.e., over two interactions in **1**–**6**):

$$\Theta = \frac{S_{Cr}(S_{Cr}+1)}{3k}\sum_j J_{ij} \qquad (1)$$

Table 4. Calculated and experimental J values for $[Cr_{10}(OR)_{20}(O_2CR')_{10}]$ (**1**–**6**).

	R	R′	χT at 300 K [$cm^3 K mol^{-1}$]	Θ[a] [K]	J[b] [cm^{-1}]	g[c]	J[c] [cm^{-1}]	PBE J[d] [cm^{-1}]	B3LYP J[e] [cm^{-1}]
1	Me	Me	17.8	+13.4±0.7	+3.7	1.98	+4.5	+10.9, +11.9[f]	–
2	Et	Me	18.8	−3.4±0.5	−1.0	1.98	−0.9	+3.1	+5.9
3	Me	Et	18.5	+0.3±0.3	+0.08	1.99	−0.37	+10.7	+7.4
4	Et	Et	17.3	−9.3±0.3	−2.6	1.94	−2.1	−17.5	−4.7
5	Me	CMe_3	18.4	+1.49±0.07	+0.41	1.98	+0.38	+4.1	–
6	Et	CMe_3	16.7	−20.2±0.5	−5.6	1.93	−5.3	−37	–

[a] From Curie–Weiss law. [b] From Weiss constant and Equation (1). [c] From fitting χT versus T. [d] Calculated by PBE numerical method using SIESTA code. [e] Calculated with B3LYP functional using a Gaussian basis set. [f] Two crystallographically independent molecules in **1**: first value for molecule containing Cr1–Cr5, second value for molecule containing Cr6–Cr10.

Method for determination of the J values: To calculate quantitatively the susceptibility for ten interacting $S=3/2$ ions we must diagonalise the Heisenberg spin–Hamiltonian matrix ($H=\Sigma -J_{ij}\hat{S}_i\hat{S}_j$) for the 116304 spin states of the cluster. Even after grouping states with the same total spin the largest matrix still has dimensions of 19425×19425, which is beyond our present computational capabilities. Therefore, in order to determine J we performed calculations on a fictitious eight-membered ring, and fitted the experimental data rescaled by a factor of 0.8. This is completely justified at high temperatures, since the exchange interactions are relatively small, as shown by the fact that the observed susceptibility values are close to those expected for ten noninteracting ions. In the case of predominantly antiferromagnetic interactions, the spin ground state is zero and the χT product tends towards zero for both ten- and eight-membered rings; the scaling procedure is expected to be a reasonable approximation. In contrast, the scaling is less valid in the ferromagnetic case, since the low-temperature limiting value of the χT value for eight ferromagnetically coupled $S=3/2$ ions (76.5 $cm^3 K mol^{-1}$) is less than that for ten ferromagnetically coupled ions rescaled by 0.8 (94.1 $cm^3 K mol^{-1}$). For this

Values of J for **1**–**6**, determined both by fitting the χT data and from the Weiss constants, are given in Table 4; the two methods are in excellent agreement with each other, which gives confidence in the results. In the discussion below we refer to the values determined from χT.

Interpretation: We have reported the magnetic data of **1** and **2** previously (see Introduction).[10] One factor which hampered our effort to characterise the intramolecular ferromagnetically coupled magnetic behaviour of **1** was the presence of an antiferromagnetic intermolecular coupling. The presence of an intermolecular interaction is easy to rationalise: a dipolar interaction between two point dipoles is expected to vary as $\propto S(S+1)/r^3$, in which S is the spin and r is the separation.[19] Therefore, for highly paramagnetic molecules (large S) there can be a significant dipolar interaction

even at relatively large distances. For example, if we treat the molecules in the crystal structure of **1** as being point dipoles with $S=15$ (due to the intramolecular ferromagnetic coupling) then we would have a dipolar interaction of $-1.2\,cm^{-1}$. This is clearly the upper limit because: 1) the Cr_{10} molecules in **1** are not point dipoles and 2) there is a Boltzmann distribution over all possible spin states (this would make the dipolar term more important as the temperature decreases, as the more paramagnetic states are preferentially populated). Nevertheless, this clearly makes the interaction derived from a fit to the experimental magnetic data of $J_{inter}=-0.26\,cm^{-1}$ feasible. The fact that we did not have to invoke such a term in the fit of **2** is not surprising—calculated χT versus T plots for **2** are insensitive to an intermolecular antiferromagnetic coupling between intramolecular antiferromagnetically coupled species ($J=-0.9\,cm^{-1}$; at 0 K only $S=0$ would be populated). A similar phenomenon to that observed for **1** has been observed in ferromagnetically coupled Cr^{III} dimers.[20]

Substitution of acetate with the slightly bigger propionate bridges in compounds **3** and **4** does not lead to a significantly increased intermolecular separation (see above) and the magnetic properties reflect this. The room-temperature values of χT are close to that expected for ten uncoupled Cr^{III} ions in both cases (18.5 and 17.3 $cm^3\,K\,mol^{-1}$ for **3** and **4**, respectively). The χT value for **3** is virtually constant down to 30 K, in agreement with a negligible Weiss constant of $\Theta=+0.3\pm0.3$ K. Below 30 K, χT decreases slowly, indicating the presence of very weak antiferromagnetic interactions. Fitting the χT data using the eight-membered ring model gives an exchange interaction of $J=-0.37\,cm^{-1}$ (Figure 3). On cooling, χT falls for **4**, consistent with weak antiferromagnetic exchange between neighbouring Cr^{III} ions. The rate of decrease is larger for **4** than for **3**, indicating stronger antiferromagnetic exchange, in agreement with the larger (more negative) Weiss temperature of $\Theta=-9.3\pm0.3$ K. The high-temperature ($T>40$ K) data for **4** can be fit with a weak antiferromagnetic interaction of $J=-2.1\,cm^{-1}$ with $g=1.94$, very similar to that observed for **2** which has a very similar χT versus T curve. Below 40 K the experimental curve decreases at a lower rate than that calculated for this exchange coupling strength, pointing to limitations of the model fit (see above). We investigated whether this could be due to the presence of more than one unique exchange interaction. For example, if two (C_2 related) J values were ferromagnetic in **4**, while the remaining eight were antiferromagnetic, an $S=3$ ground state would be expected, with a low-temperature limiting χT value of 5.9 $cm^3\,K\,mol^{-1}$. However, attempts to use exchange-coupling schemes similar to those employed to analyse the INS results on [D]**1** (see below), were unsuccessful so we limited ourselves to the simpler (single J) model above. In any case, a similar pattern is seen for the propionate-bridged compounds **3** and **4** as for the acetates **1** and **2**[10]—the ethoxide-bridged wheel is more antiferromagnetically (or less ferromagnetically) coupled than the methoxide for a given bridging carboxylate.

The magnetic behaviour of **5** is very different. Again, χT at room temperature is 18.4 $cm^3\,K\,mol^{-1}$, but then steadily increases as T is decreased, up to 26 $cm^3\,K\,mol^{-1}$ at 2 K; no maximum is observed (Figure 3). This is clearly indicative of a ferromagnetic intramolecular exchange between neighbouring Cr^{III} ions. This is supported by fitting the χ data above 15 K to a Curie–Weiss law, giving $C=18.3\,cm^3\,K\,mol^{-1}$ and a small positive (i.e., ferromagnetic) Weiss constant of $\Theta=+1.49\pm0.07$ K (Figure 4). The low-

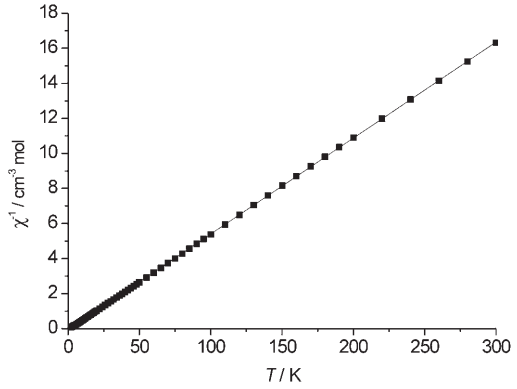

Figure 4. Plot of χ^{-1} versus T for $[Cr_{10}(OMe)_{20}(O_2CCMe_3)_{10}]$ (**5**) and the fit (solid line) to a Curie–Weiss law with $C=18.4\,cm^3\,K\,mol^{-1}$ and $\Theta=+1.49\pm0.07$ K.

temperature value of χT is much smaller than that expected for an isolated $S=15$ ground state, which is consistent with the small value of $|J|$ and consequent population of several spin states, even at 2 K. However, a magnetisation versus applied magnetic field plot fails to reach saturation, even at 6 T and 2 K (reaching ca. 17 μ_B and still increasing, Figure 5), which implies that $S=15$ is not the ground state.

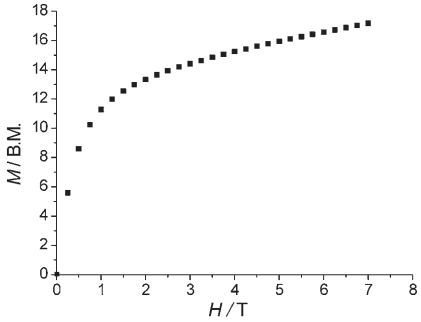

Figure 5. Magnetisation versus applied magnetic field for $[Cr_{10}(OMe)_{20}(O_2CCMe_3)_{10}]$ (**5**) at 1.8 K.

If the single J-value model is inadequate (see below) a high spin, but not the maximum possible $S=15$, ground state could result with $S=15$ as a low-lying excited state. The magnetisation would then only saturate at very high magnetic field at which the $M_S=-15$ level of the $S=15$ state crosses the lowest component of the (zero-field) ground

state. Hence, the ground-state spin of **5** is ambiguous, but must be large. However, it is clear that the cluster exhibits overall ferromagnetic coupling as evidenced by the χT data.

In **5** the intermolecular separation is significantly larger than in **1**–**4**, and this presumably helps to dampen the intermolecular interaction that is evident in **1**. The magnetic data for **5** can be fit with a weak ferromagnetic J value of $+0.38\ cm^{-1}$ (see Figure 3). Although the ferromagnetic coupling is weaker than that observed in **1**,[10] it is more evident in the χT versus T curve than is the case for **1** due to the presence of the greater intermolecular term in **1** (see above). The corresponding ethoxide complex **6** shows the strongest antiferromagnetic coupling of all of the complexes **1**–**6**, as evidenced by the rapid decrease in χT with decreasing temperature. Consequently, fitting of χT versus T gives the most negative exchange coupling constant of $J = -5.3\ cm^{-1}$, and fitting of χ^{-1} versus T gives the most negative Weiss temperature of $\Theta = -20.2 \pm 0.5$ K.

Thus, the experimental χT versus T data for **1**–**6** can be summarised (Table 4): 1) all the J values lie within a small range around $0\ cm^{-1}$, $+4.5 \geq J \geq -5.3\ cm^{-1}$, indicating that the antiferro- and ferromagnetic components of the exchange interaction are very similar in magnitude; 2) for each pair of complexes with a common carboxylate, the methoxide cluster is more ferromagnetically (or less antiferromagnetically) coupled than the ethoxide. A similar trend has been observed in the simple bis-alkoxide-bridged Cr^{III} dimers $[Cr_2(3\text{-Br-acac})_4(OR)_2]$ (3-Br-acacH = 3-bromo-2,4-pentanedionato), in which $J = -8.5$ and $-18\ cm^{-1}$ for R = Me and Et, respectively, a change of about $10\ cm^{-1}$.[21] This shift is similar to those observed between the pairs **1** and **2**, **3** and **4**, and **5** and **6**. Thus, our results are entirely in keeping with results on smaller, well-understood Cr^{III} dimers—substitution of an ethoxide group by a methoxide leads to a small shift in J to a more positive (more ferromagnetic) value. In the case of complexes **1** and **2** and **5** and **6**, the small shift happens to cross $J = 0\ cm^{-1}$ and therefore the overall coupling is switched from antiferro- to ferromagnetic (in **3**, $J \approx 0\ cm^{-1}$).

A few efforts have been made to correlate exchange coupling constants with structural parameters in $Cr(OR)_2Cr$ dimers (R = H, alkyl),[22] inspired by the successful correlation found between Cu-O-Cu angles and J in analogous Cu^{II} complexes.[23] However, the Cr–O(R) distances (r) and Cr-O(R)-Cr angles (θ) within the planar CrO_2Cr cores of $[Cr_2(3\text{-Br-acac})_4(OR)_2]$, R = Me or Et, are identical within experimental error. The change in J on changing R was initially rationalised by simple orbital-overlap arguments, as originally laid out by Hoffmann and co-workers[24] namely, the greater the electron density at the bridging atom, the greater the orbital overlap between the magnetic orbitals and the stronger the antiferromagnetic component of the exchange interaction. Thus, the larger inductive effect of an Et group versus a Me group leads to stronger antiferromagnetic exchange.[21] The same authors later argued that J was not only dependent on r and θ, but also on the dihedral angles formed between the O–R vectors and the planar CrO_2Cr cores (φ);[22a] magnetostructural correlations were developed on this basis for $Cr(OR)_2Cr$ dimers with R = H and alkyl.[22]

Extending magnetostructural correlations to higher nuclearity clusters is often hampered by the low symmetry of the clusters. The most developed correlation in cyclic clusters is Saalfrank's correlation between the Fe-O-Fe angles in the antiferromagnetically coupled Fe^{III}_6 rings $[M\subset Fe_6L_6]$ and $[M\subset Fe_8L_8]$ (M = alkali metal cation, H_3L = triethanolamine)—this study was aided by the sixfold and fourfold crystallographic symmetry, respectively, in these species.[25] Unfortunately, the comparatively low (twofold) symmetry of **1** to **5** and the range of structural parameters found within each molecule (as well as the partial disorder in the structures) makes extension of the magnetostructural correlations developed for $Cr(OR)_2Cr$ dimers from **1**–**6** difficult, and there is no evident correlation between J and any of the averaged structural parameters in Table 2.

Density functional theory calculations: Considering the lack of any clear magnetostructural correlation for **1** to **6**, we have carried out DFT calculations to provide theoretical support to the observed trends in J. Theoretical calculation of J values in high-nuclearity complexes is difficult. However, some considerable advances have been made recently in this field.[26] For example (and importantly in terms of the present study), Ruiz et al. performed calculations using Gaussian functions with hybrid B3LYP functionals on two cyclic, hexametallic Ni^{II}_6 and Cu^{II}_6 clusters, which are ferro- and antiferromagnetically coupled, respectively. The calculations not only reproduced the correct sign of J in each case, but also the correct magnitude of J to within a few cm^{-1} (cf. values derived from fitting to experimental χT vs T data).[26] On high-nuclearity systems calculation using Gaussian functions becomes hugely expensive computationally (a single calculation on a decametallic Cr^{III} cluster like **1**–**6** takes ca. three months) and the same group have proposed[27] a much faster method using the "SIESTA" code,[28] with pure Perdew–Burke–Ernzerhof (PBE) functionals and numerical basis sets. Previous work shows that correct signs and relative strengths of exchange coupling constants can be reproduced accurately by this method when applied to large clusters (although absolute values of $|J|$ tend to be slightly over estimated, compared to the Gaussian calculated values).[27,29]

Calculations on full wheels: To test the methodology applied in the SIESTA code to these high-nuclearity wheels, we performed a calculation on the ferric wheel $[Fe_{10}(OMe)_{20}(O_2CMe)_{10}]$, for which the experimental J value is well defined as $-10\ cm^{-1}$.[12] Single-point PBE numerical calculations based on the full crystal structure[13] give $J = -16\ cm^{-1}$, in good agreement in both sign and magnitude with experimental data. Therefore, we conclude that this methodology is useful to compare trends in the J values of the Cr^{III}_{10} family **1**–**6**, which are the Cr^{III} analogues of the ferric wheel but have smaller spin systems with two less unpaired electrons per metal ion.

PBE numerical calculations were performed using the full crystal structures with no simplifications or modelling. In

each case, the energy of the "ferromagnetic" $S=15$ state (E_F, all spins aligned) was calculated, as was the energy of the "antiferromagnetic" $S=0$ state (E_A, spins alternating "up" and "down" around the Cr_{10} ring) using a broken-symmetry approach. The exchange coupling constant J is then related to the energy difference by a pair-wise relationship[26a] [Eq. (2)], in which S_{Cr} is the spin of the component Cr^{III} ions ($=3/2$) and the factor ten accounts for the ten nearest neighbour interactions in the Cr_{10} ring.

$$J_{calc} = \frac{(E_A - E_F)}{10(2S_{Cr}{}^2 + S_{Cr})} \quad (2)$$

The use of Equation (2) assumes a single, nearest neighbour J value (rather than five discrete values, as would be strictly correct for a Cr_{10} ring with twofold symmetry; two discrete J values for **6**). This model is consistent with the single J models used to fit the magnetic-susceptibility data (see above).

The PBE numerically calculated J values for **1**–**6** (Table 4) are within the range $+10 > J > -37\ cm^{-1}$, in agreement with the experimental observation that the coupling is relatively weak in these clusters. For all pairs of Cr_{10} rings with a common carboxylate—**1** and **2**, **3** and **4**, and **5** and **6**—the pattern of the calculated J values is consistent with the values modelled from magnetic-susceptibility data; the methoxide-bridged species are more ferromagnetically (or less antiferromagnetically) coupled than the ethoxides.

In complex **1**, there are two crystallographically independent molecules in the crystal structure and calculations were performed on both molecules independently. For both molecules of **1** the J values are calculated to be ferromagnetic with $J=+10.9$ and $+11.9\ cm^{-1}$, respectively, in excellent agreement (correct sign and magnitude within $5\ cm^{-1}$) with the value obtained from the fitting of magnetic-susceptibility data ($+4.5\ cm^{-1}$). The fact that the calculated value is slightly larger is consistent with previous theoretical studies.[29] Note also that the two independent molecules in **1** give very similar calculated J values, as we would expect, since the structural parameters are very similar; this justifies our treatment of these molecules as identical when modelling the experimental magnetic data. Although the J value calculated for **2** is apparently the wrong sign it is within $4\ cm^{-1}$ of the experimental value and, importantly, the difference between the calculated J values of **1** and **2** is approximately $7\ cm^{-1}$, in remarkable agreement with the difference of $6\ cm^{-1}$ in the experimental values.

The experimental data for **3** imply very weak antiferromagnetic coupling ($< -1\ cm^{-1}$). Although the PBE numerical calculations on **3** predict it to be ferromagnetically coupled, the calculated value is still within about $10\ cm^{-1}$. The calculated value for **4** of $-18\ cm^{-1}$ is antiferromagnetic, in agreement with experimental value of $-2.1\ cm^{-1}$, although significantly larger. The reason for the poorer agreement, both absolute and relative, between calculated and experimental J values for **3** and **4** is unclear. Nevertheless, the calculations for **3** and **4** are in agreement with the above trends—more antiferromagnetic exchange in (ethoxide-bridged) **4** than in (methoxide-bridged) **3**. The PBE numerical calculations also support weak ferromagnetic exchange in **5** and, moreover, that this interaction is weaker than that in **1**. They also support the fact that **6** is the most strongly antiferromagnetically coupled cluster in the family. Although the DFT-calculated J values in both **4** and **6** are overestimated it is interesting to note that the ratio between the calculated and experimental J values is approximately the same between the two.

As a further test of the PBE numerical calculations, we have performed calculations using Gaussian methodology on selected complexes (**2**–**4**, see Table 4). The Gaussian and PBE numerical calculations give the same sign of J in each case, and the results for **2** and **3** are very similar (within ca. $3\ cm^{-1}$) by the two methods. In contrast, the Gaussian calculated J value for **4** is significantly smaller in magnitude than the PBE numerical value, in much better agreement with experimental data. This effect has also been observed in smaller clusters.[29]

In summary, the DFT calculations support experimentally determined trends in the magnitudes of J—a good agreement given the small experimentally observed differences between compounds **1**–**6**.

Inelastic Neutron Scattering (INS) studies of $[Cr_{10}(OCD_3)_{20}(O_2CCD_3)_{10}]$ ([D]-1): The experimental magnetic data, supported by the DFT calculations, reveal that the exchange interactions in **1** and **5** are ferromagnetic. This should lead to a very high spin ground state electronic spin, $S=15$ in the assumption of a unique J value. To probe this directly we performed INS studies on [D]**1** (**1** is easier to perdeuterate than **5**). INS allows the direct spectroscopic determination of magnetic exchange splittings. In an INS experiment incoming neutrons with an energy E_i and a momentum $\hbar\mathbf{k}_i$ exchange energy and momentum with the sample. After the scattering process the neutrons have energy E_f and momentum $\hbar\boldsymbol{k}_f$. The transferred energy $\hbar\omega = E_i - E_f$ excites the sample from one state $|\Psi_i\rangle$ into another $|\Psi_f\rangle$. The intensity of magnetic excitations generally decreases with increasing scattering vector $\boldsymbol{Q} = \boldsymbol{k}_i - \boldsymbol{k}_f$ due to the magnetic form factor.[30] Possible INS transitions are governed by the following selection rules given in Equation (3).

$$\Delta S = 0, \pm 1 \text{ and } \Delta M_S = 0, \pm 1 \quad (3)$$

The INS spectrum of [D]**1**, obtained at 1.5 K on the inverted geometry time-of-flight spectrometer IRIS, is depicted in Figure 6. The dotted line corresponds to a background accounting for thermal-diffuse scattering contributions. The spectrum after subtraction of the background is shown as a solid line. We observe peaks at 1.00(1) (I), 2.50(2) (II), 4.82(3) (III), and $5.90(2)\ cm^{-1}$ (*). On the basis of the Q (see inset Figure 6) and temperature dependence (not shown) of peaks I–III, we assign them to be of magnetic origin, while the sharp peak at $5.90\ cm^{-1}$ (*) is a temperature-independent spurious feature. All three peaks are clear-

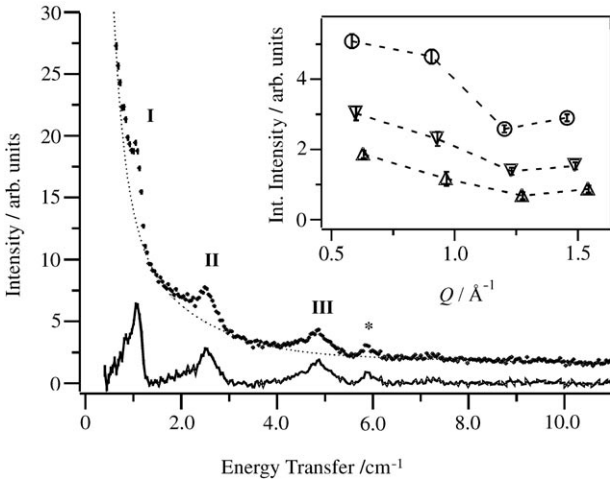

Figure 6. INS spectrum of **d-1** measured at 1.5 K on IRIS with $E_f = 14.8\ cm^{-1}$ and for detector angles $25.8° \leq 2\theta \leq 118.3°$. The solid line is the spectrum after subtraction of the thermal-diffuse scattering (dotted line). Inset: Q-dependence of the integrated intensity of peaks I (○), II (▽), and III (△); dashed lines are guides to the eye.

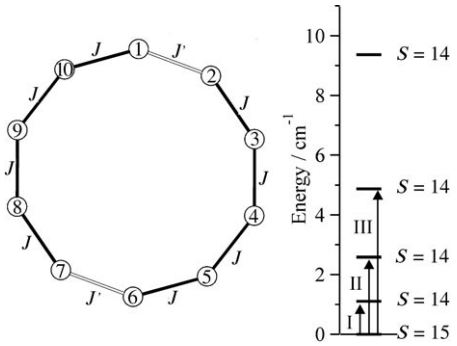

Figure 7. Coupling scheme (left) of [D]**1** for the model with $8 \times J$ and $2 \times J'$, and the calculated energy spectrum for $J = +4.5\ cm^{-1}$ and $J' = +1.1\ cm^{-1}$ (right). Vertical arrows indicate observed INS transitions.

ly asymmetric with a shoulder on the low-energy side. The experimental peak widths are up to three times as large as the instrumental resolution.

To fit the INS spectra it is necessary to explicitly consider the nature and energies of the low-lying excited-spin states and the ground state. Therefore we have calculated the low-lying states based on various J values by using MAGPACK.[31] It was not possible to get reasonable fits to the INS spectra with models for which the intracluster exchange was antiferromagnetic. Calculation of the low-lying spin states based on the model used to fit the experimental χT data for **1**—one unique ferromagnetic intracluster exchange parameter $J = +4.5\ cm^{-1}$—yields an $S = 15$ cluster ground state with two degenerate $S = 14$ states at $2.58\ cm^{-1}$ (restricting the calculations to states with $S = 15$ and $S = 14$). The next highest $S = 14$ state is at $9.36\ cm^{-1}$ and is also doubly degenerate. The state at $2.58\ cm^{-1}$ matches the energy of peak II in the INS spectrum quite well ($\Delta S = -1$), though peaks I and III remain unexplained. This result clearly shows that a model with a single J value is inadequate. Considering the C_i point symmetry of the wheel in [D]**1** this result is not surprising as there are in principal five different exchange parameters. It is evident that the INS data with three magnetic peaks do not allow the determination of five parameters. We explored models with two inequivalent parameters. Variation of $J_{12} = J_{67} = J'$, while keeping $J = +4.5\ cm^{-1}$, leads to a splitting of the degenerate $S = 14$ states. The best agreement with the observed peaks (I–III) was found for $J' = +1.1\ cm^{-1}$, as depicted in Figure 7. However, this calculation also yields an $S = 14$ state at $9.36\ cm^{-1}$, which is not observed experimentally. The above solution is the best one obtained with only two different exchange interaction parameters: models with $6 \times J$ and $4 \times J'$ were explored, but no better agreement with the observed peaks could be found. A model with $5 \times J$ and $5 \times J'$ is forbidden by symmetry.

We conclude that neither a one nor a two-parameter model can account for the three INS peaks observed. By introducing five parameters we could undoubtedly reproduce the observed peak positions by a multitude of parameter sets. Since this is pointless, there remains one important conclusion. While the magnetic data can be reasonably accounted for by a one-parameter model, the more direct, spectroscopic probe of the INS experiment shows us that this model is not adequate for **1**, consistent with the C_i molecular symmetry. The magnetically determined J value is thus an average of the five unique parameters.

The large width and asymmetry of the peaks possibly reflect a small and unresolved zero-field splitting (ZFS) with a negative D [$H_{ZFS} = D(S_z^2 - S(S+1)/3)$]. A small ZFS in the ground state of the ferromagnetically coupled examples of these clusters is consistent with preliminary EPR studies on **5**, which give a partially resolved fine structure suggesting $D \approx -0.04\ cm^{-1}$.[32] This would admix the wavefunctions of M_S levels of different S states, and thus affect the transition intensities. Intercluster interactions or an inhomogeneous distribution of cluster geometries resulting from the structural disorder could also explain the broadening of the peaks.

The agreement of INS and magnetic susceptibility data is good considering the complexity of the problem (large matrix size, low symmetry, disorder, intercluster interactions): the average exchange interaction parameter deduced from the two distinct J value models for the INS data [$J_{av} = (8J + 2J')/10 = +3.8\ cm^{-1}$] is only slightly smaller than the value obtained from magnetic susceptibility ($J = +4.5\ cm^{-1}$). Furthermore, INS data shows that the ZFS is considerably smaller than the exchange splitting.

Conclusion

In summary, we have analysed experimental variable temperature χ data for **1**–**6** to abstract J values assuming a single unique J value, by: 1) modelling χT versus T based on a Cr_8 model and scaling, and 2) from analysis of Weiss tem-

peratures. For **1** only it is necessary to include an intermolecular term to model χT. The two treatments agree well and the observed trends in J are supported by DFT-calculated values. INS studies on [D]**1** reveal that the single J-value model is not adequate, as at least three different J values are required to fit the experimental observations by this direct spectroscopic technique. The J values derived from bulk χ data are averages of the independent J values within each molecule (five for **1**–**5**, two for **6**).

Despite the lack of any clear magneostructural correlation in **1**–**6**, it is clear that, in general, the antiferro- and ferromagnetic contributions to the Cr···Cr exchange are similar, such that $|J|$ is relatively small. Furthermore, the J values unambiguously depend on the nature of the alkoxide, with the methoxides being more ferromagnetically coupled than the ethoxides. In **1** and **5** this results in an overall ferromagnetic coupling, and we have measured this directly (as opposed to fitting a magnetic susceptibility curve) in **1** by INS. The antiferromagnetic exchange in **2**, **4** and **6** must lead to $S=0$ ground states, whilst the INS data of [D]**1** is consistent with an $S=15$ ground state. We have not been able to unambiguously characterise the ground state of **5**; although it does not appear to be the maximum value of 15, S must be large because the average J value is positive. These remarkable changes in the ground state, resulting from trivial changes in chemistry, are a consequence of the fact that the average J value lies in a narrow range around zero, and in the case of **1** and **5** falls on the positive side of zero.

Despite this there is no evidence that **1** and **5** behave as SMMs at temperatures down to 1.8 K—this could either be due to a positive or small zero-field splitting in the ground spin states, or to the small magnitude of J, making it impossible to populate the ground state exclusively, even at temperatures of a few K. To this end, it would be interesting to synthesise new analogues of Cr_{10} in which the ferromagnetic exchange is greater in magnitude. If the correlation with the electron density at the bridging atoms is valid (see above), then isolating analogues of **1**–**6** with more electron-withdrawing bridges should give much more ferromagnetic J values and hence more isolated $S=15$ ground states. Such investigations are currently underway and will be reported at a later date.

Experimental Section

Magnetic measurements: Magnetic susceptibilities were measured on SQUID magnetometers (Cryogenics S600 and Quantum Design XL7) between 2 and 300 K in applied magnetic fields of 0.1 T for temperatures of 2–50 K and 1.0 T for temperatures of 40–300 K; diamagnetic corrections were applied.

INS measurements: Polycrystalline $[Cr_{10}(OCD_3)_{20}(O_2CCD_3)_{10}]$ ([D]**1**, approximately 4 g) was sealed under helium in a hollow cylinder of 23 mm outer diameter, 50 mm height, and 2 mm sample space. Experiments were performed on an inverted geometry time-of-flight IRIS spectrometer at the pulsed neutron source ISIS (Rutherford Appleton Laboratory, Chilton, UK) at four temperatures between 1.5 and 10 K. Final energy selection ($E_f=14.8\ cm^{-1}$) was achieved with the (002) reflection of pyrolythic graphite. The chosen time window allowed us to observe energy transfers from -1.6 to $11.3\ cm^{-1}$.

DFT calculations: DFT calculations were performed on the full structures of **1**–**6** by using SIESTA 1.3[28] density-functional software and PBE[33] generalised-gradient approximation functionals.[26,27,29] Only valence electrons were included in the calculations with the core being replaced by norm-conserving scalar relativistic pseudopotentials factorised in the Kleinman–Bylander form.[34] The pseudopotentials were generated by the procedure of Trouiller and Martins.[35] Numerical basis sets of triple-ζ quality with polarisation functions were used for the metal ions, and double-ζ quality with polarisation functions for the main group atoms. See reference[23] for further details.

Synthesis of $[Cr_{10}(OR)_{20}(O_2CEt)_{10}]$ [R=Me (3), Et (4)]: These complexes were prepared by heating solutions of $[Cr_3O(O_2CEt)_6(H_2O)_3]NO_3$[36] (ca. 200 mg) in ROH (ca. 10 mL) at 200 °C for 1 d followed by slow cooling ($0.1\ °C\,min^{-1}$) in 23 mL Teflon-lined Parr autoclaves; this procedure resulted in dark-green crystalline masses of the products (yields ca. 60 % for **3** and **4**). These were separated by filtration, washed with ROH and dried in air. IR (KBr) spectra of **1**–**6** contain sharp stretches at 2822–2980 cm^{-1} due to μ_2-OR.

*Data for **3***: IR(KBr): $\tilde{\nu}=2929$ (s), 2823 (s), 1553 (s), 1451 (s), 1350 (s), 687 (s), 623 (w), 537 (s), 503 cm^{-1} (m); elemental analysis calcd (%) for $Cr_{10}C_{50}H_{110}O_{40}$: C 31.5, H 5.8; found C 32.1, H 5.9. Electrospray MS in CH_2Cl_2/toluene solution: molecular ion at m/z 1872 (**3**), no other significant peaks.

*Data for **4***: IR(KBr): $\tilde{\nu}=2969$ (m), 2924 (m), 2868 (m), 1555 (s), 1456 (s), 1379 (m), 1351 (w), 1160 (w), 1105 (s), 1054 (s), 892 (s), 788 (m), 682 (s), 624 (m), 565 (s), 540 cm^{-1} (s); elemental analysis calcd (%) for $Cr_{10}C_{70}H_{150}O_{40}$: C 38.8, H 6.4; found: C 39.1, H 7.0.

Synthesis of $[Cr_{10}(OMe)_{20}(O_2CCMe_3)_{10}]$ (5): Complex **5** was prepared by heating a mixture of $[Cr_8F_8(O_2CCMe_3)_{16}]$[18] (300 mg) in MeOH (9 mL) at 200 °C for 1 d, followed by slow cooling as above. The resulting dark-green crystalline product was separated by filtration, washed with MeOH, and air dried, yield 65 %. IR (KBr): $\tilde{\nu}=2963$ (s), 2824 (s), 1544 (s), 1487 (s), 1433 (s), 1382 (s), 1231 (s), 940 (w), 904 (m), 801 (m), 788 (m), 609 (s), 511 (s), 487 cm^{-1} (w); elemental analysis calcd (%) for $Cr_{10}C_{70}H_{150}O_{40}$: C 38.9, H 6.9; found: C 39.1, 7.0.

Synthesis of $[Cr_{10}(OEt)_{20}(O_2CCMe_3)_{10}]$ (6): Complex **6** was prepared by an analogous reaction to that of **5**, using EtOH in place of MeOH, yield 53 %. IR(KBr): $\tilde{\nu}=2964$ (s), 2927 (m), 2871 (m), 1549 (s), 1486 (s), 1433 (s), 1382 (s), 1363 (s), 1230 (s), 1162 (w), 1110 (s), 1055 (s), 898 (s), 800 (w), 787 (s), 611 (s), 539 cm^{-1} (s); elemental analysis calcd (%) for $Cr_{10}C_{90}H_{190}O_{40}$: C 43.3, H 6.3; found: C 44.4, H 7.9.

Synthesis of compound $[Cr_{10}(OCD_3)_{20}(O_2CD_3)_{10}]$ ([D]1): Compound [D]**1** can be prepared by an analogous route to **1**[10] from $[Cr_3O(O_2CD_3)_6(H_2O)_3]Cl$ in CD_3OH at 200 °C. However, we found that we could obtain better yields of [D]**1** starting from $[Cr_3O(O_2CD_3)_6(H_2O)_3](O_2CCD_3)$, based on the preparation reported by Jayasooriya et al.[37] for $[Cr_3O(O_2CD_3)_6(H_2O)_3]X$ (X=Cl or NO_3). $[Cr_3O(O_2CMe)_6(H_2O)_3](O_2CMe)$ was prepared by addition of a solution of NaOH (4.0 g) in minimum H_2O to a solution of $CrCl_3{\cdot}6H_2O$ (8.8 g) in H_2O (50 mL) with rapid stirring. The resulting precipitate was filtered off and air dried, before being dissolved in glacial acetic acid (6.4 g) in a large evaporating dish. The green solution was warmed until most of the solvent evaporated and a crystalline solid product was obtained. Elemental analysis calcd (%) for $Cr_3C_{14}H_{27}O_{18}$: C 20.4, H 3.8, Cr 20.2; found C 20.8, H 4.1, Cr 19.3. $[Cr_3O(O_2CD_3)_6(H_2O)_3](O_2CCD_3)$ was prepared by an analogous route, substituting CD_3CO_2D for CH_3CO_2H. Note that because the terminal water molecules are not incorporated into the final product [D]**1**, it was not necessary to use D_2O in this preparation.

Crystalline samples of **1** obtained from $[Cr_3O(O_2CMe)_6(H_2O)_3](O_2CMe)$ gave identical analyses and unit cells to those reported previously.[10] A sample of [D]**1** was prepared by heating $[Cr_3O(O_2CD_3)_6(H_2O)_3](O_2CCD_3)$ (200 mg) in CD_3OD (10 mL) at 200 °C for 1 d in a 23 mL Teflon-lined Parr autoclave, followed by slow cooling to give a dark-green crystalline product, yield 20 %. The CD_3OD filtrate was recovered after each reaction, distilled, and reused in repeated reactions in

order to obtain the approximately 4 g of [D]**1** necessary for INS measurements. IR (KBr): $\tilde{\nu}$ = 2205 (m), 2124 (w), 2061 (s), 1436 (s), 1443 (s), 1104 (s), 1028 (s), 926 (w), 847 (w), 661 (m), 533 (s), 460 cm^{-1} (m).

X-ray crystallography: Data were measured on a Bruker SMART diffractometer with a CCD area detector for **5** and **6**, and a Rigaku RAXIS rotating anode with image-plate detector for **2** and **3**, with graphite monochromators ($Mo_{K\alpha}$). Absorption corrections were applied to **5** and **6** (multiscan), but not to **3** or **4**. Structure solution (by direct methods) and refinement were performed with SHELXS L-97. Refinement of F^2 was against all reflections. Details of data collection and refinement are given in Table 1.

The asymmetric unit of **3** contains half the molecule, with the other half related by a centre of symmetry. The atoms C1F, C1G and C1J were disordered over two sites each, the occupancies of which were constrained to sum to 1.0 with isotropic thermal parameters constrained to be equal, and restraints on their bond lengths. H atoms were included in calculated positions, and the non-H atoms, except those of the disordered atoms, were refined anisotropically. The *R* factor was rather high which might be due to crystal twinning, with *b* and *c* reversed. A twinning matrix was included, and the fraction of each component refined to 0.5119:0.4881, this improved the R value by about 1%. The asymmetric unit of **4** consists of half the molecule. The thermal motion of all atoms was high, especially for the C atoms. In some cases there was disorder over two sites, with occupancies constrained at 0.5 for each site. Some methyl C atoms were not located. H atoms were included in calculated positions when possible, and the Cr and O atoms were refined anisotropically; other non-H atoms were refined isotropically. Some restraints were used on the bond lengths and angles between the C atoms. The asymmetric unit of **5** contains half the cluster. Some of the *t*Bu and Me groups are disordered over two sites, the occupancies of which were constrained to sum to 1.0. The non-H atoms were refined anisotropically, with restraints on geometric and thermal parameters of the C atoms. H atoms bonded to C were included in calculated positions. The asymmetric unit of **6** contains one quarter molecule. One pivalate was disordered over two sites the occupancies of which were constrained to sum to 1.0; similarly, C24 was disordered over two sites. The thermal motion of the Et groups C6, C7 and C15, C16 were very high and attempts were made to split these groups into two disordered components, but this did not improve the atomic displacement parameters of these atoms. Therefore, they were not split in the final rounds of refinement and were refined with restraints on their geometry. Non-H atoms were refined anisotropically, with restraints on those of the C atoms. H atoms were included in calculated positions.

CCDC-281843–281846 contains the supplementary crystallographic data for this paper. These data can be obtained free of charge from The Cambridge Crystallographic Data centre via www.ccdc.cam.ac.uk/data_request/cif.

Acknowledgements

We thank the EPSRC, the Leverhulme Trust, the EC (HPRN-CT-1999–00012/TMR network "Molnanomag", and MRTN-CT-2003–504880 "QuEMolNa") and the Swiss National Science Foundation for financial support. We also thank the UK Computational Chemistry Facility (UKCCF) for access to computing resources on Columbus/Proton at the Rutherford Appleton Laboratories (RAL), and the ISIS facility at the RAL for the award of beamtime on IRIS for INS measurements.

[1] R. E. P. Winpenny, *Adv. Inorg. Chem.* **2003**, *52*, 1.
[2] A. L. Dearden, S. Parsons, R. E. P. Winpenny, *Angew. Chem.* **2001**, *113*, 155; *Angew. Chem. Int. Ed.* **2001**, *40*, 151.
[3] a) A. Caneschi, D. Gatteschi, C. Sangregorio, R. Sessoli, L. Sorace, A. Cornia, M. A. Novak, C. Paulsem, W. Wernsdorfer, *J. Magn. Magn. Mater.* **1999**, *200*, 182; b) D. Gatteschi, R. Sessoli, A. Cornia, *Chem. Commun.* **2000**, 725.
[4] F. K. Larsen, E. J. L. McInnes, H. El Mkami, J. Overgaard, S. Piligkos, G. Rajaraman, E. Rentschler, A. A. Smith, V. Boote, M. Jennings, G. A. Timko, R. E. P. Winpenny, *Angew. Chem.* **2003**, *115*, 105; *Angew. Chem. Int. Ed.* **2003**, *42*, 101.
[5] a) F. Meier, D. Loss, *Phys. Rev. B* **2001**, *64*, 224411/1; b) F. Meier, J. Levy, D. Loss, *Phys. Rev. B* **2003**, 68, 134417.
[6] a) E. Rentschler, D. Gatteschi, A. Cornia, A. C. Fabretti, A.-L. Barra, O. I. Shchegolikhina, A. A. Zhdanov, *Inorg. Chem.* **1996**, *35*, 4427; b) G. L. Abbati, A. Cornia, A. C. Fabretti, A. Caneschi, D. Gatteschi, *Inorg. Chem.* **1998**, *37*, 1430.
[7] a) A. J. Blake, C. M. Grant, S. Parsons, J. M. Rawson, R. E. P. Winpenny, *J. Chem. Soc. Chem. Commun.* **1994**, 2363; b) E. K. Brechin, O. Cador, A. Caneschi, C. Cadiou, S. G. Harris, S. Parsons, M. Vonci, R. E. P. Winpenny, *Chem. Commun.* **2002**, 1860.
[8] a) R. Sessoli, H-L. Tsai, A. R. Schake, S. Wang, J. B. Vincent, K. Folting, D. Gatteschi, G. Christou, D. N. Hendrickson, *J. Am. Chem. Soc.* **1993**, *115*, 1804; b) R. Sessoli, D. Gatteschi, A. Caneschi, M. A. Novak, *Nature* **1993**, *365*, 141.
[9] H. Andres, R. Basler, A. J. Blake, C. Cadiou, G. Chaboussant, C. M. Grant, H. U. Güdel, M. Murrie, S. Parsons, C. Paulsen, F. Semadini, V. Villar, W. Wernsdorfer, R. E. P. Winpenny, *Chem. Eur. J.* **2002**, *8*, 4867.
[10] E. J. L. McInnes, C. Anson, A. K. Powell, A. J. Thomson, S. Poussereau, R. Sessoli, *Chem. Commun.* **2001**, 89.
[11] a) A. S. Batsanov, G. A. Timko, Y. T. Strutchkov, N. V. Gérbéléu, K. M. Indrichan, *Koord. Khim.* **1991**, *17*, 662; b) F. E. Mabbs, E. J. L. McInnes, M. Murrie, S. Parsons, G. M. Smith, C. C. Wilson, R. E. P. Winpenny, *Chem. Commun.* **1999**, 643; c) S. Parsons, A. A. Smith, R. E. P. Winpenny, *Chem. Commun.* **2000**, 579.
[12] K. L. Taft, C. D. Delfs, G. C. Papaefthymiou, S. Foner, D. Gatteschi, S. J. Lippard, *J. Am. Chem. Soc.* **1994**, *116*, 823.
[13] C. Benelli, S. Parsons, G. A. Solan, R. E. P. Winpenny, *Angew. Chem.* **1996**, *108*, 1957; *Angew. Chem. Int. Ed. Engl.* **1996**, *35*, 1825.
[14] R. H. Laye, M. Murrie, S. Ochsenbein, A. Bell, S. J. Teat, J. Raftery, H. U. Güdel, E. J. L. McInnes, *Chem. Eur. J.* **2003**, *9*, 6215.
[15] a) N. V. Gérbéléu, Y. T. Struchkov, G. A. Timko, A. S. Batsanov, K. M. Indrichan, G. A. Popovich, *Dokl. Chem.* **1991**, *313*, 1459; b) I. M. Atkinson, C. Benelli, M. Murrie, S. Parsons, R. E. P. Winpenny, *Chem. Commun.* **1999**, 285; c) M. Eshel, A. Bino, I. Felner, D. C. Johnston, M. Luban, L. L. Miller, *Inorg. Chem.* **2000**, *39*, 1376; d) M. Eshel, A. Bino, *Inorg. Chim. Acta* **2002**, *329*, 45; e) J. van Slageren, R. Sessoli, D. Gatteschi, A. A. Smith, M. Helliwell, R. E. P. Winpenny, A. Cornia, A-L. Barra, A. G. M. Jansen, E. Rentschler, G. A. Timco, *Chem. Eur. J.* **2002**, *8*, 277.
[16] a) S. L. Heath, A. K. Powell, *Angew. Chem.* **1992**, *104*, 191; *Angew. Chem. Int. Ed. Engl.* **1992**, *31*, 191; b) Z. J. Zhong, H. Seino, Y. Mizobe, M. Hidai, A. Fujishima, S. Ohkoshi, K. Hashimoto, *J. Am. Chem. Soc.* **2000**, *122*, 2952; c) J. Larionova, M. Gross, M. Pilkington, H. Andres, H. Stoekli-Evans, H. U. Güdel, S. Decurtins, *Angew. Chem.* **2000**, *112*, 1667; *Angew. Chem. Int. Ed.* **2000**, *39*, 1605; d) D. M. Low, L. F. Jones, A. Bell, E. K. Brechin, E. J. L. McInnes *Angew. Chem.* **2003**, *115*, 3911; *Angew. Chem. Int. Ed.* **2003**, *42*, 3781; e) M. Murugesu, M. Habrych, W. Wernsdorfer, A. Khalil, G. Christou, *J. Am. Chem. Soc.* **2004**, *126*, 4766.
[17] R. H. Laye, E. J. L. McInnes, *Eur. J. Inorg. Chem.* **2004**, 2811.
[18] N. V. Gérbéléu, Yu. T. Struchkov, G. A. Timco, A. S. Batsanov, K. M. Indrichan, G. A. Popovich, *Dokl. Akad. Nauk SSSR* **1990**, *313*, 1459.
[19] A. Abragam, B. Bleaney, *Electron Paramagnetic Resonance of Transition Ions*, Clarendon, Oxford (UK), **1970**, Chapter 3.
[20] C. Reber, H. U. Gudel, L. Spiccia, W. Marty, *Inorg. Chem.* **1987**, *26*, 3186.
[21] E. D. Estes, R. P. Scaringe, W. E. Hatfield, D. J. Hodgson, *Inorg. Chem.* **1977**, *16*, 1605.
[22] a) J. Glerup, D. J. Hodgson, E. Pederson, *Acta Chem. Scand.A* **1983**, *37*, 161; b) "Magneto-Structural Correlations in Exchange Coupled Systems": D. J. Hodgson, *NATO ASI Ser. C*, **1983**, *140*, 497; c) M. F. Charlot, O. Khan, M. Drillon, *Chem. Phys.* **1982**, *70*, 177; d) S. De-

curtins, H.-U. Güdel, *Inorg. Chem.* **1982**, *21*, 3598; e) S. Emori, K. Obata, W. Mori, *ITE Lett. Batt. New Tech. Med.* **2000**, *1*, 938.
[23] V. H. Crawford, H. W. Richardson, J. R. Wasson, D. J. Hodgson, W. E. Hatfield, *Inorg. Chem.* **1976**, *15*, 2107.
[24] P. J. Hay, J. C. Thibeault, R. Hoffmann, *J. Am. Chem. Soc.* **1975**, *97*, 4884.
[25] O. Waldmann, R. Koch, S. Schromm, J. Schülein, P. Müller, I. Bernt, R. W. Saalfrank, F. Hampel, E. Balthes, *Inorg. Chem.* **2001**, *40*, 2986.
[26] a) E. Ruiz, A. Rodríguez-Fortea, J. Cano, S. Alvarez, P. Alemany, *J. Comput. Chem.* **2003**, *24*, 982; b) E. Ruiz, *Struct. Bonding* **2004**, *113*, 71; c) E. Ruiz, J. Cano, S. Alvarez, A. Caneschi, D. Gatteschi, *J. Am. Chem. Soc.* **2003**, *125*, 6791.
[27] E. Ruiz, A. Rodríguez-Fortea, J. Cano, S. Alvarez, *J. Phys. Chem. Solids* **2004**, *65*, 799.
[28] J. M. Soler, E. Artacho, J. D. Gale, A. Garcia, J. Junquera, P. Ordejon, D. Sanchez-Portal, *J. Phys.: Condens. Matter* **2002**, *14*, 2745.
[29] E. Ruiz, S. Alvarez, A. Rodríguez-Fortea, P. Alemany, Y. Pouillon, C. Massobrio in *Magnetism: Molecules to Materials, Vol. 2* (Eds.: J. S. Miller, M. Drillon), Wiley-VCH, Weinheim, **2001**.
[30] A. Furrer, P. Böni, in *Seventh Summer School on Neutron Scattering* (Ed.: A. Furrer), World Scientific, Zuoz, Switzerland, **1999**, p. 11.
[31] J. J. Borras-Almenar, J. M. Clemente-Juan, E. Coronado, B. S. Tsukerblat, *J. Comput. Chem.* **2001**, *22*, 985.
[32] S. Sharmin, A. Ardavan, S. J. Blundell, A. I. Coldea, E. J. L. McInnes, D. Low, *Appl. Phys. Lett.* **2005**, *86*, 032507.
[33] J. Perdew, K. Burke, M. Enzerhof, *Phys. Rev. Lett.* **1996**, *77*, 3865.
[34] L. Kleinman, D. M. Bylander, *Phys. Rev. Lett.* **1982**, *48*, 1425.
[35] N. Trouiller, J. L. Martins, *Phys. Rev. B* **1991**, *43*, 1993.
[36] R. D. Cannon, R. P. White, *Prog. Inorg. Chem.* **1988**, *36*, 195.
[37] U. A. Jayasooriya, R. D. Cannon, R. P. White, J. A. Stride, R. Grinter, G. J. Kearley, *J. Chem. Phys.* **1993**, *98*, 9303.

Received: August 25, 2005
Published online: November 28, 2005

